Active contours for multi-region image segmentation with a single level set function

Anastasia Dubrovina, Guy Rosman and Ron Kimmel

Computer Science Department, Technion - IIT, Haifa, Israel
{nastyad, rosman, ron}@cs.technion.ac.il

Abstract. Segmenting the image into an arbitrary number of parts is at the core of image understanding. Many formulations of the task have been suggested over the years. Among these are axiomatic functionals, which are hard to implement and analyze, while graph-based alternatives impose a non-geometric metric on the problem.
We propose a novel approach to tackle the problem of multiple-region segmentation for an arbitrary number of regions. The proposed framework allows generic region appearance models while avoiding metrication errors. Updating the segmentation in this framework is done by level set evolution. Yet, unlike most existing methods, evolution is executed using a *single non-negative* level set function, through the Voronoi Implicit Interface Method for a multi-phase interface evolution. We apply the proposed framework to synthetic and real images, with various number of regions, and compare it to state-of-the-art image segmentation algorithms.

1 Introduction

Image segmentation plays an important role in object detection and classification, scene understanding, action classification, and other visual information analysis processes. In this paper we consider active contour approaches, which have been proven to be very successful for that goal. These include edge-based methods [15, 5, 18, 6] , region-based techniques [21, 8, 10, 13] , and combined approaches [37, 24, 28], to mention just a few.

Several approaches have been suggested for numerical computation of region boundaries. These include explicit spline evolution [15], level set evolution [23, 5], graph-cuts [3, 27, 12], and continuous convex optimization [25, 7]. Among these, the level set framework provides a significant amount of flexibility in the design of the segmentation criterion. While being naturally suitable for variable topology of the regions, this framework has been extended to accommodate different assumptions on the image and its structure. These include various appearance models [13, 20, 22, 1], and different shape priors [16, 11, 26].

However, the level set framework is geared towards two-region image segmentation. To alleviate this limitation, various methods were developed; most of them require managing *multiple* level set functions. Some associate a level set function with each image region, and evolve these functions in a coupled manner

[36, 35, 29]. Others perform hierarchical segmentation, by iteratively splitting previously obtained regions using the conventional level set framework [33, 4]. These methods too require coupled level set evolution, so that the resulting regions do not develop gaps or overlaps. It is also possible to use a smaller number of level set functions, say n, and segment an image into 2^n regions [34]. Another approach was recently suggested in [17]. It uses a single level set function, similar to the proposed approach. However, when evolving the contour, it requires managing multiple auxiliary level set functions, so that no gaps/overlaps are created.

Other approaches to multi-region image segmentation either use a discrete labeling problem formulation and solve it using graph-cuts [27, 12], or perform convex relaxation [25, 7]. These methods are less easy to adapt for arbitrary segmentation functionals, in terms of both data and geometry priors. In addition, such approaches usually require knowing the number of regions a priori. Yet another method for image segmentation is by mean-shift clustering [10]. This approach does not, however, allow flexible choice of shape priors or arbitrary probability models.

We propose a new level set method for multiple region image segmentation. It overcomes previous challenges and allows segmenting images with arbitrary number of regions using various image appearance models. For this purpose we utilize a novel level set framework for multi-phase, or multi-region, interface evolution, named the Voronoi Implicit Interface Method (VIIM), which was introduced by Saye and Sethian in [30]. According to it, evolution is performed using a *single* non-negative level set function, while implicitly dealing with regions merging and splitting, and naturally handling arbitrary topological structures such as triple junctions.

Our main contributions can be summarized as follows: first, we review the axiomatic formulation of the multi-region image segmentation problem as an energy functional minimization. Specifically, we consider energy terms used in image segmentation based on region statistics, and extend them to the context of multiple regions. We then derive the active contour evolution equation minimizing the above energy functional, formulate it as a level set evolution problem, and solve it by utilizing the VIIM level set framework. The proposed approach does not require knowing the number of the regions in the image or their statistics a priori, and produces good segmentation results for various initial contours.

The structure of the paper is as follows: we begin by reviewing the Voronoi Implicit Interface Method, which is the numerical basis for our approach, in Section 2. In Section 3 we describe the main ideas that underlie the proposed method. We shortly review the multi-region segmentation model, for which we derive the corresponding level set evolution equation in terms of the VIIM framework, and describe prominent segmentation priors that fit within the suggested framework. In Section 4 we present segmentation results of the proposed approach, and compare it to state-of-the-art methods. Section 5 concludes the paper and describes potential extensions of the proposed framework.

2 Review of the Voronoi Implicit Interface Method

The VIIM was recently suggested for the solution of interface propagation problems with arbitrary number of phases, or regions, in m-dimensional Euclidean space. In 2D, the interface separating between different phases is a curve, possibly with multiple junctions. In 3D, the interface consists of two-dimensional surfaces. Illustrations of 2D and 3D interfaces can be found in [30].

The interface propagation is performed using a *single* non-negative level set function $\phi(\mathbf{x}), \mathbf{x} \in \mathbb{R}^m$, given by the unsigned distance from the interface Γ, and defined on a fixed regular grid. The propagation is governed by the equation

$$\phi_t = F_{ext} \left| \nabla \phi \right|, \tag{1}$$

where F_{ext} is the extension of the interface propagation speed F to the whole m-dimensional region. The examples in [30] include curvature and mean curvature flows, as well as physical simulations of the dynamics of dry foams.

The central idea of the VIIM is as follows: assume we are given a zero level set of a function ϕ, and a velocity F defined along it. We can extend this velocity to the neighboring level sets in a smooth manner, to obtain the extension velocity F_{ext} and apply Eq. (1). Then, two evolving ϵ-level sets will always encapsulate the evolving zero level set they are adjacent to. Moreover, the ϵ-level sets of ϕ are simple curves, without multiple-junction points, and their evolution is well defined. Thus, the evolved ϵ-level sets of the level set function can be used to reconstruct the evolving interface, which is assumed to lie at an equal distance from the two ϵ-level sets adjacent to it. It is calculated using the Voronoi regions of the ϵ-level sets.

In order to evolve the interface as described above, Saye and Sethian suggested the following three step-algorithm.

1. Evolve the level set function ϕ by solving Eq. (1).
2. Find the ϵ-level sets of the new function. Reconstruct the interface Γ to be the intersections of the Voronoi regions of the ϵ-level sets, where $\phi(\mathbf{x}) < \epsilon$. Update the level set function ϕ using the reconstructed interface Γ.
3. Update the propagation speed function F; return to 1.

The VIIM is formulated in terms of a general interface velocity F, and thus it is applicable to various interface evolution problems utilizing the level set approach. Below, we show how it can be employed for multiple regions image segmentation, where the active contour acts as an interface, and the regions it defines are the phases in the VIIM notation.

3 Multi-region image segmentation

A general energy functional describing an active contour model is given by

$$E(C) = E_{data}(C) + \mu E_{reg}(C). \tag{2}$$

The data term $E_{data}(C)$ is determined by the region-based image intensity model, for instance [21, 8, 13, 20], etc. In this paper we demonstrate region-based terms that rely on two specific image models - the piecewise-constant model of [21, 8] and a more general *Gaussian mixture model* (GMM). The regularization term $E_{reg}(C)$ is determined by the properties of the segmenting contour, and may depend on the contour alone [15, 21], or incorporate image information as well [5, 6]. The minimizing flow is derived from (2) using methods from calculus of variations, namely the active contour evolution is proportional to the first variation of the above energy functional.

3.1 Region-competition model with geodesic active contours regularization

Here, we consider a modified version of the region competition model of Zhu and Yuille [37], with added *geodesic active contour* (GAC) regularization term

$$E(C, \{\alpha_i\}) = \sum_i \iint_{\Omega_i} -\log P\left(I(x,y)|\alpha_i\right) dxdy + \mu \oint_C g(C(s))ds, \qquad (3)$$

where $I(x,y)$ is the image to be segmented, defined on a 2D domain Ω. The contour C divides the image domain into non-overlapping regions $\{\Omega_i\}_i$, such that $\Omega = \{\bigcup_i \Omega_i\} \bigcup C$. In the data term, $P\left(z|\alpha_i\right)$ is the probability distribution function of the image intensity values in region Ω_i, with corresponding parameters α_i. In the GAC term, $g(x,y)$ is the edge indicator function. Following [6], in this work we used $g(x,y) = \left(1 + \left|\nabla \hat{I}\right|^2\right)^{-1}$, where $\hat{I}$ is a smooth version of I. For color images we used $g(x,y)$ suggested in [28]: we treat the image as a 5-dimensional manifold $(x, y, \mathrm{R}(x,y), \mathrm{G}(x,y), \mathrm{B}(x,y))$ with metric $g_{\mu\nu}(x,y)$, so that the edge indicator function becomes $g(x,y) = \det\left(g_{\mu\nu}(x,y)\right)^{-1}$.

We perform alternating minimization: for a fixed contour C, for each region Ω_i we calculate the optimal parameters maximizing the image probability in that region

$$\alpha_i^* = \arg\max_{\alpha_i} \prod_{(x,y)\in\Omega_i} P\left(\alpha_i|I(x,y)\right), \quad \forall i. \qquad (4)$$

Then, for fixed region probability distribution parameters, the active contour evolution minimizing the energy $E(C, \{\alpha_i\})$ is given by

$$C_t = -\frac{\delta E}{\delta C} = \sum_{i\in N(x,y)} \log P\left(I|\alpha_i\right) \mathbf{n}_i + \mu\left(\kappa g - \langle \nabla g, \mathbf{n}\rangle\right)\mathbf{n}. \qquad (5)$$

For some $(x,y) \in C$, $N_i(x,y)$ denotes the set of indices of the regions Ω_j adjacent to C at (x,y). In each region, the normal $\mathbf{n}_i$ is defined such that it points outwards of the region Ω_i. The first term of the minimizing flow is obtained by differentiating the functional $E_{data}(C)$, as shown in [37]. The second term is the well known explicit geodesic active contour flow, obtained by differentiating the

regularization term in Eq. 3. The above evolution rule is well-defined for (x, y) lying on a contour segment defining a boundary between two regions Ω_i and Ω_j, for which $|N(x, y)| = 2$. We will denote such contour segments by C_{ij}.

The traditional methods, described in the introduction, require using multiple level set functions to perform the above evolution implicitly. In this work we suggest to exploit the advantages of the Voronoi implicit interface method for this purpose. The next section describes how to adapt the evolution rule Eq. (5) to be applicable within the VIIM framework. We would also like to note that the above formulation is general and may be applied for various models of image intensity probability distribution. In order to demonstrate this we apply the proposed method to two such models – Gaussian probability distribution with constant variance, leading to piecewise constant image segmentation functional [21, 8], and a more elaborated Gaussian mixture model (GMM). Both models will be described in details in Section 3.3.

3.2 Contour evolution using the VIIM

In terms of the VIIM framework, the contour (interface) velocity $F(x, y)$ is well defined for points lying along a boundary between two regions, and is given by

$$F(x, y) = \left[\log P\left(I(x, y)|\alpha_i\right) - \log P\left(I(x, y)|\alpha_j\right)\right] + \mu\left(\kappa g - \langle \nabla g, \mathbf{n}_i \rangle\right), \quad (6)$$

in the direction $\mathbf{n}_i$, for $(x, y) \in C_{ij}$. According to the VIIM formulation, the contour velocity F needs to be extended to the neighboring level sets of the level set function $\phi(x, y)$, to create $F_{ext}(x, y)$. We observe that a straight forward extension of (6) produces a velocity profile with discontinuities at the boundaries of the Voronoi regions of different contour segments. This is also related to the fact that the interface velocity F is not well defined at the junction points.

Alternatively, we suggest to evolve the level sets of $\phi(x, y)$ in each region according to the local information of that region alone. Thus, the extension velocity, used to evolve the level set function according to Eq. (1), is defined by

$$F_{ext}(x, y) = \log P\left(I(x, y)|\alpha_i\right) + \mu \mathrm{div}\left(g(x, y)\frac{\nabla\phi}{|\nabla\phi|}\right), \quad (x, y) \in \Omega_i. \quad (7)$$

Proposition 1. *Assume that the level set function is given by an unsigned distance function from the evolving contour, and the parameters $\{\alpha_i\}$ are fixed. For $\epsilon \ll 1$, the VIIM framework with the extension velocity $F_{ext}(x, y)$ defined in Eq. (6) will move every regular point (x, y) on the contour in the direction of the velocity $F(C(x, y))\mathbf{n}_i$ (6) minimizing the energy functional $E(C)$ in Eq. (3).*

The suggested extension velocity F_{ext} (7) evolves the contour points along the same direction as $F(C(x, y))$ (if not by the same amount). Our experiments show that the suggested extension velocity produces valid segmentation results. Particularly, for the two-region piecewise constant problem, the results obtained with the proposed method are similar to those obtained using the original formulation of Chan-Vese [8]. Proof of Prop. 1 is given in the accompanying supplementary material.

The proposed approach can be summarized as follows: assume we are given an initial contour C_0 and the corresponding unsigned distance level set function $\phi(x, y)$.

1. Calculate extension velocity in each region using Eq. (7). Evolve the function $\phi(x, y)$ using the obtained velocity according to the evolution equation (1).
2. Extract the ϵ-level sets of the evolved level set function. Calculate the Voronoi regions of these ϵ-level sets in the narrow band $\{(x, y) : \phi(x, y) < \epsilon\}$, and reconstruct the evolved contour C as the collection of the boundaries between these Voronoi regions, as suggested by [30]. Perform re-distancing: re-calculate the unsigned level set function $\phi(x, y)$ using the new contour C.
3. Stop the evolution if a pre-defined stopping criterion was met; otherwise, return to Step 1.

3.3 Image segmentation models

Piecewise constant model: In this case we assume Gaussian probability distribution, given by $I \sim \mathcal{N}(c_i, \sigma_i^2)$ in region Ω_i. Further simplified by an assumption $\sigma_i = \sigma_j, \forall i, j$, the energy functional becomes

$$E_{MR}(C, \{c_i\}) = \sum_i \iint_{\Omega_i} (I(x, y) - c_i)^2 \, dxdy + \mu \oint_C g(C(s))ds. \tag{8}$$

The above is a modified version of the piecewise constant Mumford-Shah energy functional [21], in the sense that the regularization term is given by the geodesic active contours model (GAC). The contour C now separates multiple regions, denoted by Ω_i, and may have multiple-junction points. For $N = 2$ and $g = 1$, (8) is the well known Chan-Vese functional [8].

According to Equation (7), the extension velocity F_{ext} in the region Ω_i is given by

$$F_{ext}(x, y) = -(I(x, y) - c_i) + \mu \mathrm{div}\left(g(x, y)\frac{\nabla\phi}{|\nabla\phi|}\right), \quad (x, y) \in \Omega_i. \tag{9}$$

For a given contour C, the optimal mean intensity values in each region, c_i^*, are given by

$$c_i^* = \frac{\iint_{\Omega_i} I(x, y)dxdy}{\iint_{\Omega_i} dxdy}. \tag{10}$$

Gaussian mixture model: Here, we model image intensity values in each region using the Gaussian mixture model [19], which have been successfully applied to various signal analysis tasks; specifically, in computer vision it was used for tracking [32], MR image segmentation [14], background substraction [38], etc. In GMM, the intensity probability distribution in region Ω_i is modeled by a weighted sum of m Gaussians, each with mean $c_i^{(j)}$ and covariance matrix $\sigma_i^{(j)} I$,

$$P(z|\alpha_i) = \sum_{j=1}^{m} \lambda_i^{(j)} \mathcal{N}\left(z \mid c_i^{(j)}, \sigma_i^{(j)} I\right), \tag{11}$$

where $\mathcal{N}\left(z \mid c_i^{(j)}, \sigma_i^{(j)} I\right)$ is the j^{th} component of the Gaussian mixture in the region Ω_i. The results shown in the next section were obtained with $m = 6$.

The extension velocity (7) becomes

$$F_{ext}(x,y) = \log\left[\sum_{j=1}^{m} \lambda_i^{(j)} \mathcal{N}\left(I(x,y) | c_i^{(j)}, \sigma_i^{(j)} I\right)\right] + \mu \text{div}\left(g(x,y)\frac{\nabla\phi}{|\nabla\phi|}\right), \quad (x,y) \in \Omega_i. \qquad (12)$$

The optimal model parameters α_i^*, where $\alpha_i = \left\{\lambda_i^{(j)}, c_i^{(j)}, \sigma_i^{(j)}\right\}_{j=1}^{m}$, are then calculated as suggested in Eq. (4), using an Expectation Maximization (EM) algorithm [19].

Finally, note that though the above problem formulation is given in terms of the image intensity values, other image representations can be easily utilized in the suggested framework, depending on a specific segmentation problem.

4 Experimental results

In this section we present segmentation results obtained with the proposed method for different types of images, and compare them to the results obtained using the convex relaxation method of Chambolle and Pock [7]. In all our experiments, the image intensity values were normalized to the range $[0, 1]$. The algorithm parameters were $\mu \in [0.02, 0.1]$, the time step $dt = [25, 50]$, and $\epsilon = 0.1$. In order to prevent over-segmentation, we united separate regions with similar region statistics, as a part of Step 2 of the algorithm. For the piecewise constant model, we united regions with mean intensity value difference smaller than some threshold (if not stated explicitly, $T = 0.1$ was used).For color images, we used the maximal difference among the three color channels. For the GMM, we used the L_2-distance between sampled three-dimensional (for color images) probability distributions. The level set function evolution (1) was performed using the forward Euler scheme. To perform re-distancing and Voronoi region calculation we used the fast marching method [31], efficiently initialized as suggested in [9]. Both the ϵ-level set and the evolved contour extraction were performed with sub-pixel precision. It should be also noted that the width of the ϵ-level sets influences the size of the smallest feature that the algorithm is able to segment. To capture small features one may up-sample the image before the segmentation, similar to the technique used in [2].

It is important to note the computational efficiency of the proposed method. Typically, significant parts of the evolution can be performed in a narrow-band fashion. Specifically, the update of the piecewise-constant model, as well as the M-step of the EM estimation for the Gaussian mixture model can be performed incrementally, keeping the same complexity of the 2-region active contours scheme. The expectation step of the EM algorithm, however, requires computation over the entire image domain. Exploring efficient implementation aspects such as incremental update of the expectation is left for future work.

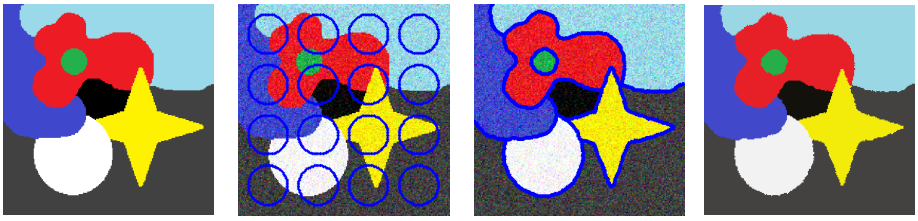

Fig. 1. Segmentation of noisy synthetic color image with overlapping objects. Left to right: the original image, noisy image with the initial contour, region boundaries obtained using the piecewise constant model, piecewise constant segmentation.

In our first experiment, we applied the algorithm with the piecewise constant model to a noisy synthetic image with several overlapping regions, with of triple-junction boundary intersections. The segmentation result is shown in Fig. 1.

Fig. 2 presents a comparison of the proposed method, and the convex relaxation method of Chambolle and Pock [7], minimizing the piecewise constant Mumford-Shah functional [21], closely related to the piecewise constant model described above. To evaluate [7] we used the code published by the authors, with the algorithm parameters chosen to obtain visually optimal results: isotropic TV, simple relaxation, initialization with k-means clustering, $K = 8$, and $\lambda = 5.0$. We further compared the proposed method with the graph-cut based approach of [12], which we applied to the piecewise constant model. We iterated segmentation and model-estimation, as described in [12], with initial model parameters obtained with k-means clustering, and the algorithm parameters chosen to obtain optimal results with the same number of regions as the two previous algorithms: 8-connected neighborhood, $\lambda = 1/16$, with label cost set to be zero. From examining the images in Fig. 2, (d),(e) and (f), we observe that in this case the three methods produce comparable results.

Fig. 3 presents segmentation results obtained with the piecewise constant variant of the proposed method, and different values of the threshold T. Specifically, increasing T results in more regions being deemed similar and merged during the evolution process, thus producing less detailed segmentation. The above results were compared to segmentation obtained with [7] and [12], with algorithms' parameters chosen to produce similar number of regions as the proposed method. [12] was used with 8-connected neighborhood, with the initial parameters obtained using k-means clustering for both methods. The results are shown in Fig. 4. We observe that in this case both latter approaches fail to segment one of the objects, namely, the orange candy, and associate part of it with the background.

Fig. 5 presents the segmentation result obtained with the proposed method for an image from the Berkeley Segmentation Dataset[1], along with the ground-truth segmentation. Our method captures the main objects in the image, though it does not detect small image features, such as thin lines and tiny structures.

[1] `http://www.eecs.berkeley.edu/Research/Projects/CS/vision/bsds/`

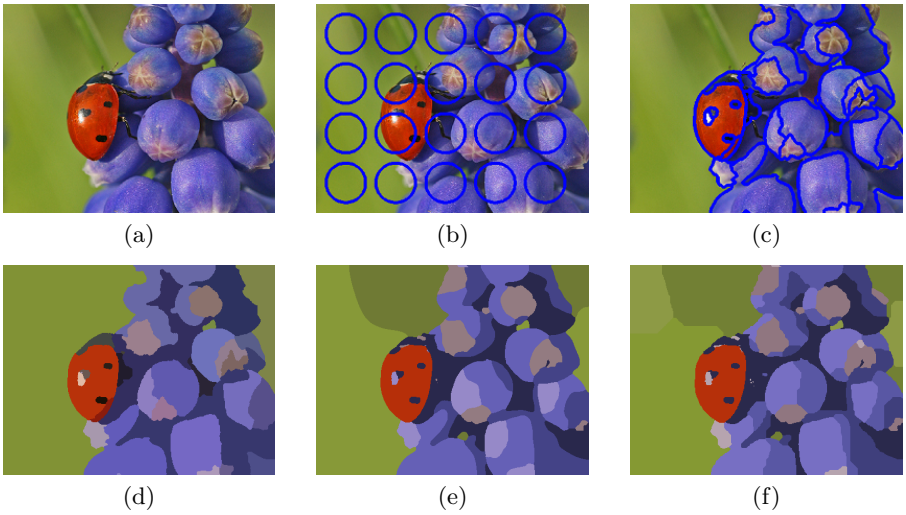

Fig. 2. Comparison of the proposed method using the multi-region piecewise constant model, the convex relaxation approach of [7], and the graph-cut based method of [12]. (a) The original image. (b) Initial contour. (c) Region boundaries detected by our method. (d) Regions detected by our method, colored according to their mean intensity values. (e), (f) The results of [7] and [12], accordingly.

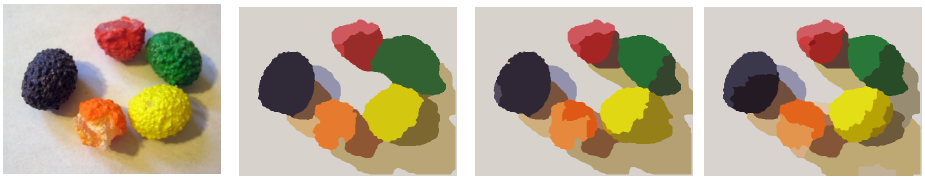

Fig. 3. Segmentation results obtained with the proposed method using different values of the absolute intensity difference T.

This can be overcome by up-sampling the image prior to the segmentation [2]. It also should be noted that some of the object boundaries provided in the ground-truth segmentation and not detected by the proposed method, may be found only using a prior knowledge of the object structure.

In Fig. 6 we demonstrate the application of multi-region piecewise constant model (8) for tracking in a thermal camera video sequence, where the segmentation obtained for k-th frame is used to initialize the algorithm in frame $k + 1$. The proposed approach seemlessly allows multiple target tracking in the video sequence. In Fig. 7 we demonstrate the segmentation obtained using the proposed method with Gaussian mixture model. The introduction of more expressive region appearance models naturally allows us to segment more complex images.

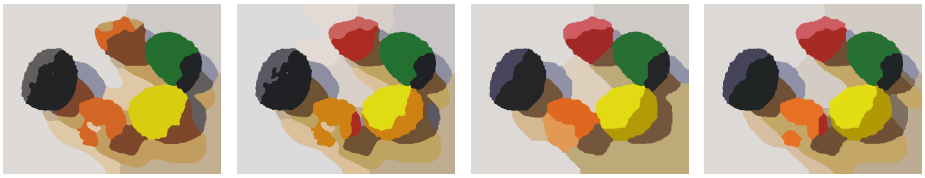

(a) $(K, \lambda) = (12, 6)$ (b) $(K, \lambda) = (16, 8)$ (c) $\lambda = 1/8$ (d) $\lambda = 1/16$

Fig. 4. Segmentation results obtained with (a), (b) [7] and (c), (d) [12], with different algorithm parameters.

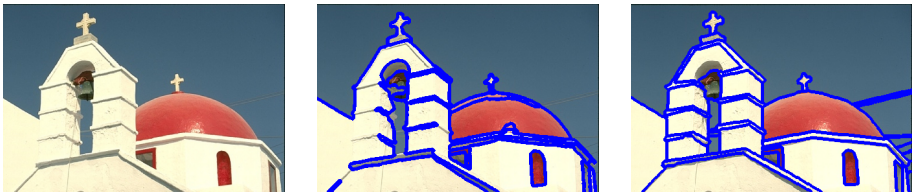

Fig. 5. Segmentation of an image from the Berkeley Segmentation Dataset. Left to right: the original image, region boundaries obtained using our method with piecewise constant model, ground-truth segmentation.

5 Conclusions and future work

In this paper we addressed the problem of segmenting an image into an arbitrary number of regions using a novel active contours formulation. The proposed framework allows utilizing various region appearance priors and employs the new Voronoi implicit interface method in order to treat multiple regions in a uniform manner, while avoiding metrication errors. Finally, we demonstrated that the proposed method works well on challenging images from various data sets and applications.

Acknowledgements

The authors thank J.A. Sethian of UC Berkeley for intriguing discussions and introducing the VIIM to our group. This research was supported by European Community's FP7-ERC program, grant agreement no. 267414.

References

1. A. Adam, R. Kimmel, and E. Rivlin. On scene segmentation and histograms-based curve evolution. *IEEE-TPAMI*, 31(9):1708–1714, 2009.
2. T. Amiaz, E. Lubetzky, and N. Kiryati. Coarse to over-fine optical flow estimation. *Pattern Recognition*, 40(9):2496 – 2503, 2007.
3. Y. Boykov, O. Veksler, and R. Zabih. Fast approximate energy minimization via graph cuts. *IEEE-TPAMI*, 23(11):1222–1239, Nov. 2001.

Fig. 6. Tracking in a thermal camera video sequence from a surveillance camera. Yellow contours show the region boundaries in four frames from the sequence. The leftmost subfigure demonstrates the initial contour.

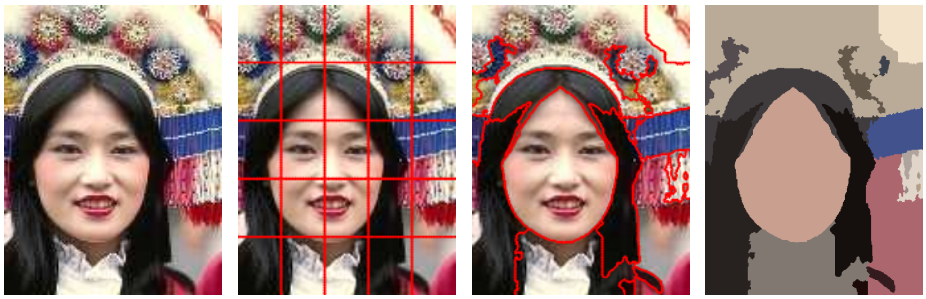

Fig. 7. Segmentation obtained using the Gaussian mixture to model image intensity probability density. Left to right: the original image, the initial contour, region boundaries obtained by our method, regions colored according to their mean intensity values.

4. T. Brox and J. Weickert. Level set segmentation with multiple regions. *IEEE-TIP*, 15(10):3213–3218, 2006.
5. V. Caselles, F. Catté, T. Coll, and F. Dibos. A geometric model for active contours in image processing. *Numerische Mathematik*, 66(1):1–31, 1993.
6. V. Caselles, R. Kimmel, and G. Sapiro. Geodesic active contours. *IJCV*, 22(1):61–79, 1997.
7. A. Chambolle and T. Pock. A first-order primal-dual algorithm for convex problems with applications to imaging. *JMIV*, 40(1):120–145, 2011.
8. T. Chan and L. Vese. Active contours without edges. *IEEE-TIP*, 10(2):266–277, 2001.
9. D. L. Chopp. Some improvements of the fast marching method. *SIAM Journal on Scientific Computing*, 23(1):230–244, 2001.
10. D. Comaniciu and P. Meer. Mean shift: A robust approach toward feature space analysis. *IEEE-TPAMI*, 24(5):603–619, May 2002.
11. D. Cremers, T. Kohlberger, and C. Schnörr. Shape statistics in kernel space for variational image segmentation. *Pattern Recognition*, 36(9):1929–1943, 2003.
12. A. Delong, A. Osokin, H. N. Isack, and Y. Boykov. Fast approximate energy minimization with label costs. *IJCV*, 96(1):1–27, 2012.
13. D. Freedman and T. Zhang. Active contours for tracking distributions. *IEEE-TIP*, 13(4):518–526, 2004.
14. H. Greenspan, A. Ruf, and J. Goldberger. Constrained Gaussian mixture model framework for automatic segmentation of MR brain images. *Medical Imaging, IEEE Transactions on*, 25(9):1233–1245, 2006.
15. M. Kass, A. Witkin, and D. Terzopoulos. Snakes: active contour models. *IJCV*, 1(4):321–331, 1988.

16. M. E. Leventon, W. E. L. Grimson, and O. D. Faugeras. Statistical shape influence in geodesic active contours. In *CVPR*, pages 1316–1323, 2000.
17. B. Lucas, M. Kazhdan, and R. Taylor. Multi-object spring level sets (muscle). *MICCAI*, pages 495–503, 2012.
18. R. Malladi, J. Sethian, and B. Vemuri. Shape modeling with front propagation: A level set approach. *IEEE-TPAMI*, 17(2):158–175, 1995.
19. G. McLachlan and D. Peel. *Finite mixture models*. Wiley-Interscience, 2000.
20. O. Michailovich, Y. Rathi, and A. Tannenbaum. Image segmentation using active contours driven by the Bhattacharyya gradient flow. *IEEE-TIP*, 16(11):2787–2801, 2007.
21. D. Mumford and J. Shah. Optimal approximations by piecewise smooth functions and associated variational problems. *Communications on pure and applied mathematics*, 42(5):577–685, 1989.
22. K. Ni, X. Bresson, T. Chan, and S. Esedoglu. Local histogram based segmentation using the Wasserstein distance. *IJCV*, 84(1):97–111, 2009.
23. S. Osher and J. Sethian. Fronts propagating with curvature-dependent speed: algorithms based on Hamilton-Jacobi formulations. *J. of Computational Physics*, 79(1):12–49, 1988.
24. N. Paragios and R. Deriche. Geodesic active regions: A new framework to deal with frame partition problems in computer vision. *Journal of Visual Communication and Image Representation*, 13(1-2):249–268, 2002.
25. T. Pock, T. Schoenemann, G. Graber, H. Bischof, and D. Cremers. A convex formulation of continuous multi-label problems. *ECCV*, pages 792–805, 2008.
26. T. Riklin-Raviv, N. Kiryati, and N. Sochen. Prior-based segmentation by projective registration and level sets. In *ICCV*, volume 1, pages 204–211. IEEE, 2005.
27. C. Rother, V. Kolmogorov, and A. Blake. "grabcut": interactive foreground extraction using iterated graph cuts. *ACM Trans. Graph.*, 23(3):309–314, Aug. 2004.
28. C. Sagiv, N. Sochen, and Y. Zeevi. Integrated active contours for texture segmentation. *IEEE-TIP*, 15(6):1633–1646, 2006.
29. C. Samson, L. Blanc-Féraud, G. Aubert, and J. Zerubia. A level set model for image classification. *IJCV*, 40(3):187–197, 2000.
30. R. Saye and J. Sethian. The Voronoi Implicit Interface Method for computing multiphase physics. *PNAS*, 108(49):19498–19503, 2011.
31. J. Sethian. A fast marching level set method for monotonically advancing fronts. *Proceedings of the National Academy of Sciences*, 93(4):1591, 1996.
32. C. Stauffer and W. Grimson. Adaptive background mixture models for real-time tracking. In *CVPR*, volume 2. IEEE, 1999.
33. A. Tsai, A. Yezzi Jr, and A. Willsky. Curve evolution implementation of the Mumford-Shah functional for image segmentation, denoising, interpolation, and magnification. *IEEE-TIP*, 10(8):1169–1186, 2001.
34. L. Vese and T. Chan. A multiphase level set framework for image segmentation using the Mumford and Shah model. *IJCV*, 50(3):271–293, 2002.
35. A. Yezzi Jr, A. Tsai, and A. Willsky. A statistical approach to snakes for bimodal and trimodal imagery. In *ICCV*, volume 2, pages 898–903. IEEE, 1999.
36. H. Zhao, T. Chan, B. Merriman, and S. Osher. A variational level set approach to multiphase motion. *J. of Computational Physics*, 127(1):179–195, 1996.
37. S. Zhu and A. Yuille. Region competition: unifying snakes, region growing, and Bayes/MDL for multiband image segmentation. *IEEE-TPAMI*, 18(9):884–900, 1996.
38. Z. Zivkovic. Improved adaptive Gaussian mixture model for background subtraction. In *ICPR*, volume 2, pages 28–31. IEEE, 2004.